



A Novel Actinobacterial Cutinase Containing a Noncatalytic Polymer-Binding Domain

Kofi Abokitse,^{a*} Stephan Grosse,^a Hannes Leisch,^{a§} Christopher R. Corbeil,^b Florence Perrin-Sarazin,^c Peter C. K. Lau^{a,d}

^aAquatic and Crop Resource Development, National Research Council Canada, Montréal, Canada

^bHuman Health Therapeutics Research Centre, National Research Council Canada, Montréal, Canada

^cIndustrial Materials Institute, National Research Council Canada, Boucherville, Canada

^dMicrobiology & Immunology, McGill University, Montréal, Canada

ABSTRACT The single putative cutinase-encoding gene from the genome of *Kineococcus radiotolerans* SRS30216 was cloned and expressed in *Escherichia coli* as a secreted fusion protein, designated YebF-KrCUT, where YebF is the extracellular carrier protein. The 294-amino-acid sequence of KrCUT is unique among currently characterized cutinases by having a C-terminal extension that consists of a short (Pro-Thr)-rich linker and a 55-amino-acid region resembling the substrate binding domain of poly(hydroxybutyrate) (PHB) depolymerases. Phylogenetically, KrCUT takes a unique position among known cutinases and cutinase-like proteins of bacterial and fungal origins. A modeled structure of KrCUT, although displaying a typical α/β hydrolase fold, shows some unique loops close to the catalytic site. The 39-kDa YebF-KrCUT fusion protein and a truncated variant thereof were purified to electrophoretic homogeneity and functionally characterized. The melting temperatures (T_m) of KrCUT and its variant KrCUT206 devoid of the putative PHB-binding domain were established to be very similar, at 50 to 51°C. Cutinase activity was confirmed by the appearance of characteristic cutin components, C₁₆ and C₁₈ hydroxyl fatty acids, in the mass chromatograms following incubation of KrCUT with apple cutin as the substrate. KrCUT also efficiently degraded synthetic polyesters such as polycaprolactone and poly(1,3-propylene adipate). Although incapable of PHB depolymerization, KrCUT could efficiently bind PHB, confirming the predicted characteristic of the C-terminal region. KrCUT also potentiated the activity of pectate lyase in the degradation of pectin from hemp fibers. This synergistic effect is relevant to the enzyme retting process of natural fibers.

IMPORTANCE To date, only a limited number of cutinases have been isolated and characterized from nature, the majority being sourced from phytopathogenic fungi and thermophilic bacteria. The significance of our research relates to the identification and characterization of a unique member of the microbial cutinases, named KrCUT, that was derived from the genome of the Gram-positive *Kineococcus radiotolerans* SRS30216, a highly radiation-resistant actinobacterium. Given the wide-ranging importance of cutinases in applications such as the degradation of natural and synthetic polymers, in the textile industry, in laundry detergents, and in biocatalysis (e.g., transesterification reactions), our results could foster new research leading to broader biotechnological impacts. This study also demonstrated that genome mining or prospecting is a viable means to discover novel biocatalysts as environmentally friendly and biotechnological tools.

KEYWORDS α/β fold hydrolase, cutinase, biotechnology, enzyme technology, microbial world, *Kineococcus*, biopolymer degradation

Cutinases (EC 3.1.1.74) are hydrolytic enzymes that degrade cutin, a component of the plant cuticle that, in addition to waxes, constitute the outermost continuous membrane or "skin" of the primary parts of higher plants (1). Cutin is a polyester, largely composed of cross-linked saturated C₁₆ (palmitic) acids and unsaturated C₁₈ fatty acids; the actual

Citation Abokitse K, Grosse S, Leisch H, Corbeil CR, Perrin-Sarazin F, Lau PCK. 2022. A novel actinobacterial cutinase containing a noncatalytic polymer-binding domain. *Appl Environ Microbiol* 88:e01522-21. <https://doi.org/10.1128/AEM.01522-21>.

Editor Nicole R. Buan, University of Nebraska—Lincoln

© Crown copyright 2022. The government of Australia, Canada, or the UK ("the Crown") owns the copyright interests of authors who are government employees. The [Crown Copyright](#) is not transferable.

Address correspondence to Peter C. K. Lau, peter.lau@mcgill.ca.

*Present address: Kofi Abokitse, Ozymes Inc., Trois-Rivières, QC, Canada.

§Present address: Hannes Leisch, Novartis Pharma Stein AG, Stein, Switzerland.

Received 28 July 2021

Accepted 19 October 2021

Accepted manuscript posted online

27 October 2021

Published 11 January 2022

composition depends on the plant species (2). The cuticle primarily protects plants from water loss or other environmental stresses, thereby acting as a formidable barrier.

Cutinases have been found predominantly in phytopathogenic fungi as secreted enzymes to facilitate entry into the host plant. The prototypical cutinase is the cutinase (FsCUT) derived from *Fusarium solani* f. sp. *pisi* (also known as *Nectria haematococca*), which infects peas (3, 4). This enzyme plays a role in plant pathogenesis as a virulence factor, although not exclusively, since hydrophobic surface binding proteins, called hydrophobins, are also involved (5). FsCUT is a 230-amino-acid enzyme synthesized with a 31-amino-acid signal peptide, with the mature, secreted portion having a molecular mass of 21,600 Da (4). Its structure belongs to the α/β class of hydrolases (ABH) containing the classical Ser-His-Asp triad (S120, H188, and D175) for effecting catalysis (6), a machinery that is known to drive at least 17 other reactions including lipases (7, 8). A distinguishing structural feature of cutinase versus that of a lipase or other hydrolases is the absence of a lid or flap over the active site, which is needed for interfacial activation of lipases (9).

The first set of bacterial cutinase-encoding genes, derived from a moderate thermophilic soil bacterium, *Thermobifida fusca* (formerly *Thermomonospora fusca*), was only reported in 2008 (10). Since then, the majority of cloned genes have come from related thermophilic actinomycete species such as *Thermobifida cellulosilytica* (11), *Thermobifida alba* (12, 13), and *Thermomonospora curvata* (14). Structures of these proteins as well as a metagenome-derived leaf-branch compost cutinase (LCC) have been determined (15; reviewed in reference 16).

All other fungal cutinases that have been characterized biochemically and at the molecular level, including those sequences that have been designated cutinase-like proteins (CULPs), e.g., the seven homologs in *Mycobacterium tuberculosis*, are members of the ABH structural class (16–18). These proteins, while sharing a similar predicted functional site like that of the well-characterized FsCUT, are not able to hydrolyze cutin, the natural substrate of a cutinase (17). On the other hand, many other cutinase-like hydrolases have been isolated and investigated for the ability to degrade polyethylene terephthalate (PET) and related polyesters (19, 20; reviewed in references 21 and 22). Otherwise, cutinases have wide-ranging applications that include esterification, transesterification in synthesis, stereoselective catalysis, food processing, laundry and detergents, textiles in the modification of fabrics, and more (3, 18, 23–27).

As cloned bacterial cutinase-encoding genes are relatively scarce compared to those of fungal sources, this study was conducted to characterize a new cutinase (KrCUT), genome mined from *Kineococcus radiotolerans* SRS30216, a highly radiation-resistant actinobacterium originally isolated from a nuclear waste site at the Savannah River in Aiken, SC (28). We describe the novel domain organization of the KrCUT protein, ease of protein secretion in *Escherichia coli*, properties of the purified KrCUT and a truncated variant, and its possible use in the processing of natural fibers.

RESULTS

Amino acid sequence analysis and phylogenetic tree of KrCUT. The predicted 294-amino-acid sequence of KrCUT derived from gene locus [YP_001363838.1](#) (29) is remotely identical in sequence (17.3%) to the prototypical cutinase sequence of *Fusarium* (FsCUT) and to various characterized cutinases or CULPs in the realm of 22 to 25.5%. However, beyond the *Kineococcus* species such as *Kineococcus vitellinus* and *Kineococcus indalonis*, the top hits are those of the potential cutinases of *Microlunatus sagamiharensis* (formerly *Friedmanniella sagamiharensis*) and *Microlunatus flavus*, showing a sequence identity of 67 to 69%. Potential cutinase candidates from other high-G+C Gram-positive actinobacteria, such as *Klenkia marina* and *Cellulomonas bogoriensis*, score in the range of 61 to 72% sequence identity. A multiple-sequence alignment of a short list of selected sequences is shown in Fig. 1, highlights of which are presented below.

KrCUT is predicted to have a modular domain organization consisting of a 33-amino-acid signal peptide, a catalytic domain, and the presence of a C-terminal extension, made up of a 16- to 17-residue Pro/Thr-rich linker, and a putative polymer-binding domain of 55 residues (Fig. 1A). The mature portion of KrCUT, comprising 261 amino acids with a calculated

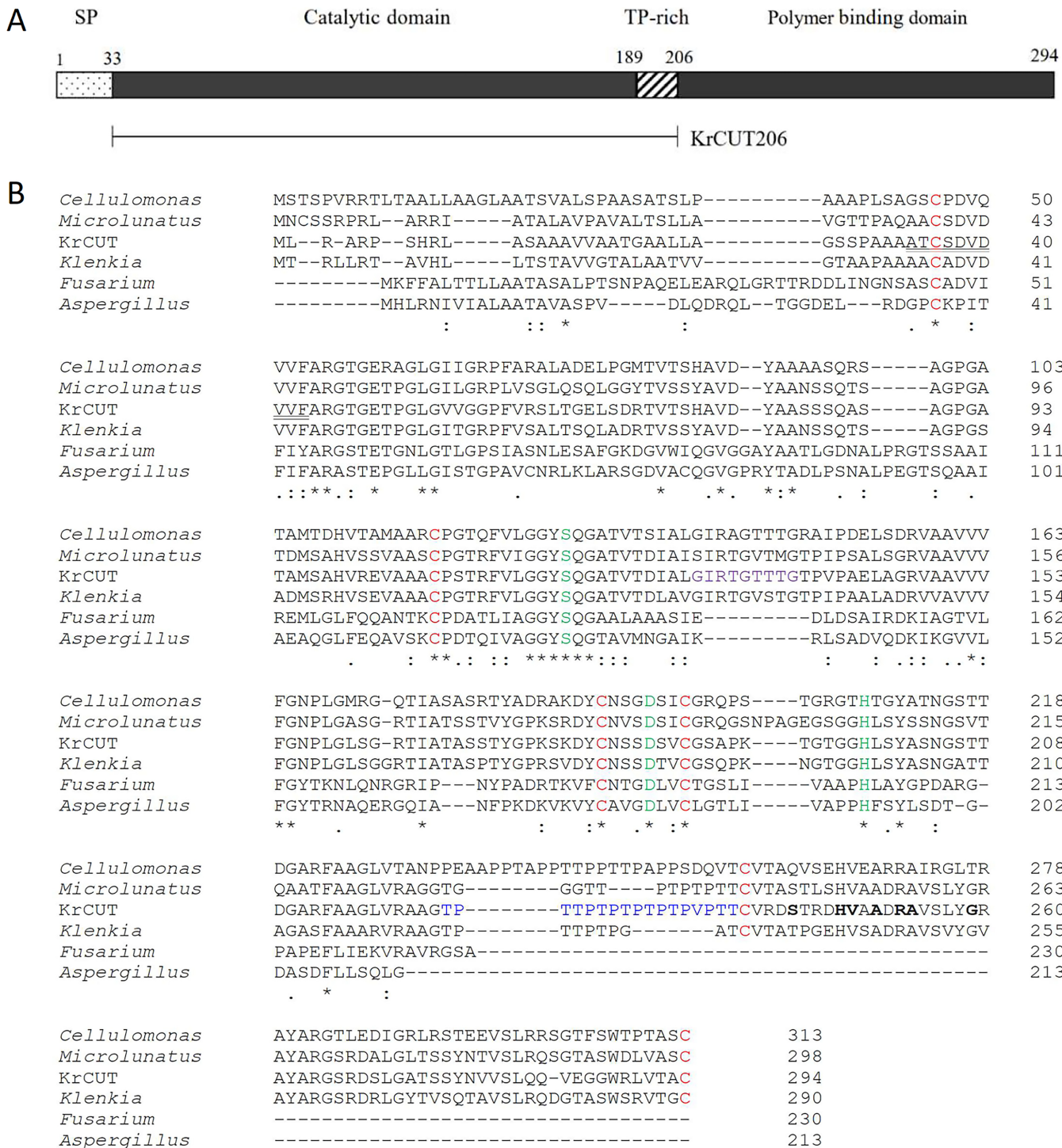


FIG 1 (A) Schematic representation of the domain organization of KrCUT. SP, signal peptide; TP-rich, threonine-proline-rich linker. KrCUT206 is truncated KrCUT without the polymer-binding domain. Cloning of the KrCUT and KrCUT206-encoding genes is facilitated by the primers described in Table 1. (B) Clustal Omega (1.2.4) multiple-sequence alignment of KrCUT from *K. radiotolerans* (YP_001363838.1) with *Cellulomonas bogoriensis* (WP_156968314), *Microlunatus sagamiharensis* (WP_197680654), *Klenkia marina* (WP_207798241), *Fusarium solani* (AAA3335.1 and 1CUS), and *Aspergillus oryzae* RIB40 (3GBS). Asterisks indicate totally conserved amino acids, the catalytic triad residues are highlighted in green and conserved C (cysteine) in red, double-underlined residues in KrCUT indicate the experimentally determined amino acid sequence, the 9-amino-acid sequence in purple is the insertion in KrCUT as described in the text, the threonine-proline-rich sequence is shown in blue, and the boldfaced amino acid residues in the C terminus are conserved residues of the SBD-binding sequence of known PHB depolymerases.

molecular mass of 26,067 Da, is in agreement with the experimentally determined value of 29 kDa (see below). A conserved protein domain search indicated pfam01083 cutinase, a member of the α/β hydrolase (ABH) superfamily cl21494. Among the conserved sequence residues is the serine hydrolase pentapeptide GxSxG motif (G83-Y84-S85-Q86-G87), of which

S85 is part of the catalytic triad, the other two catalytic residues being D151 and H165 (Fig. 1A). Unless otherwise specified, the numbers refer to the positions of the amino acid residues starting from the N terminus of the mature protein. KrCUT contains six cysteines at positions 3, 74, 147, 154, 207, and 261 at the extreme C terminus. Flanked by two cysteines, this C-terminal 55-amino-acid region contains a substrate binding domain (SBD)-like sequence (STRDHVAADRAVSLYG) observed in all SBDs of known PhaZ [poly(hydroxybutyrate) (PHB) depolymerase] sequences (SNYAHv-AgRA—gG [30, 31]). This stretch is well conserved among the KrCUT-related actinobacterial sequences (Fig. 1B and Fig. 2).

A phylogenetic tree analysis of 56 sequences (Fig. 2) revealed that KrCUT is in a distinct clade separate from those of *Mycobacterium* cutinases and CULPs, the well-studied fungal cutinases (e.g., FsCUT and *Aspergillus oryzae* cutinase [AoCUT]), and several *Thermobifida* sequences (e.g., TfU0882 and TfU0883). The polyethylene phthalate (PET)-degrading cutinases (e.g., leaf-branch compost cutinase [LCC] of an unknown genus and the mesophilic PETase of *Ideonella sakaiensis*) are well separated from the KrCUT cluster, which is nested with a representative of an oomycete (e.g., *Phytophthora infestans*) (32).

Modeled KrCUT structure. Through a BLAST protein search using the Protein Data Bank (PDB) and correlating it with results from a text search for cutinase, four top structures (PDB codes **1CEX**, **4PSE**, **4OYY**, and **1CUU**; see Table S1 in the supplemental material) corresponding to cutinases of *F. solani*, *Humicola insolens*, *Trichoderma reesei*, and a mutant of *F. solani*, respectively, were used as templates for building a homology model using SWISS-MODEL (SM) (33). The resulting models were then analyzed using PROCHECK and MolProbity to assess the model quality. For details, see Materials and Methods and Table S1 and Table S2 in the supplemental material.

Figure 3 is a two-dimensional structure plot of KrCUT displaying a typical α/β hydrolase fold with 5 β -sheets, surrounded by 4 α -helices. The conserved residues of the catalytic triad are localized in the indicated loops of α 3 helix/ β 3 sheet and β 5 sheet/ α 4 helix. Within the modeled catalytic domain, the presence of two disulfide bonds, the first between C3 and C74 and the second between C147 and C154, is consistent with the known disulfide bonds seen in other cutinases, such as C31-C109 and C171-C178 in the crystal structure of *F. solani* (PDB code **1CEX**). Shown as a cartoon sphere, the relatively short C-terminal polymer/SBD has no structural template with high similarity in the presently available database. Hence, a third disulfide bond cannot be established but is most likely present.

An overlay of modeled KrCUT and *F. solani* crystal structures is shown in Fig. S1, and of concern is the loop protruding into solvent. This loop corresponds to a 9-residue insertion (GIRTGTTG) between G96 and G104 of KrCUT that protrudes into the solvent for all generated models. As of this writing, there are no available cutinase structures that contain an insertion at the same location. However, a BLAST search of the entire cutinase sequence suggested that a loop in acetylxyran esterase (PDB code **1BS9**) from C101 to A114 may be similar (Fig. S2). This loop, instead of protruding into solvent, folds back and forms one end of the catalytic site (Fig. S3). Overall, the local similarity in the stems (± 4 residues on either side of the insertion [Fig. S3]) is higher between KrCUT and acetylxyran esterase (PDB code **1BS9**) (62.5%) than for the KrCUT templates used for building the homology model (cutinase [PDB code **1CEX**], 37.5%; *H. insolens* cutinase [PDB code **4OYY**], 50.0%; *T. reesei* cutinase in complex with a C11Y4 phosphonate inhibitor [PDB code **4PSE**], 37.5%; and cutinase A199C mutant [PDB code **1CUU**], 37.5%). Due to the high similarity in the stem region of acetylxyran esterase (PDB code **1BS9**) versus other cutinases, the loop was used as an initial template for the 9-residue insertion. The acetylxyran esterase loop was truncated at the tip and mutated to the KrCUT sequence. In addition to the 9-residue insertion, the conformations of the helix prior to and after were grafted to ensure that the joint was ideal. These grafted models (SM and SM + loop graft [LG]) were analyzed by PROCHECK and the MolProbity web server (Table S2) to assess their quality. Overall, the grafted models have a slightly lower percentage of angles in disallowed Ramachandran space yet fewer in the core region along with slightly lower G-factor values. Like the PROCHECK numbers, MolProbity scores are slightly higher than

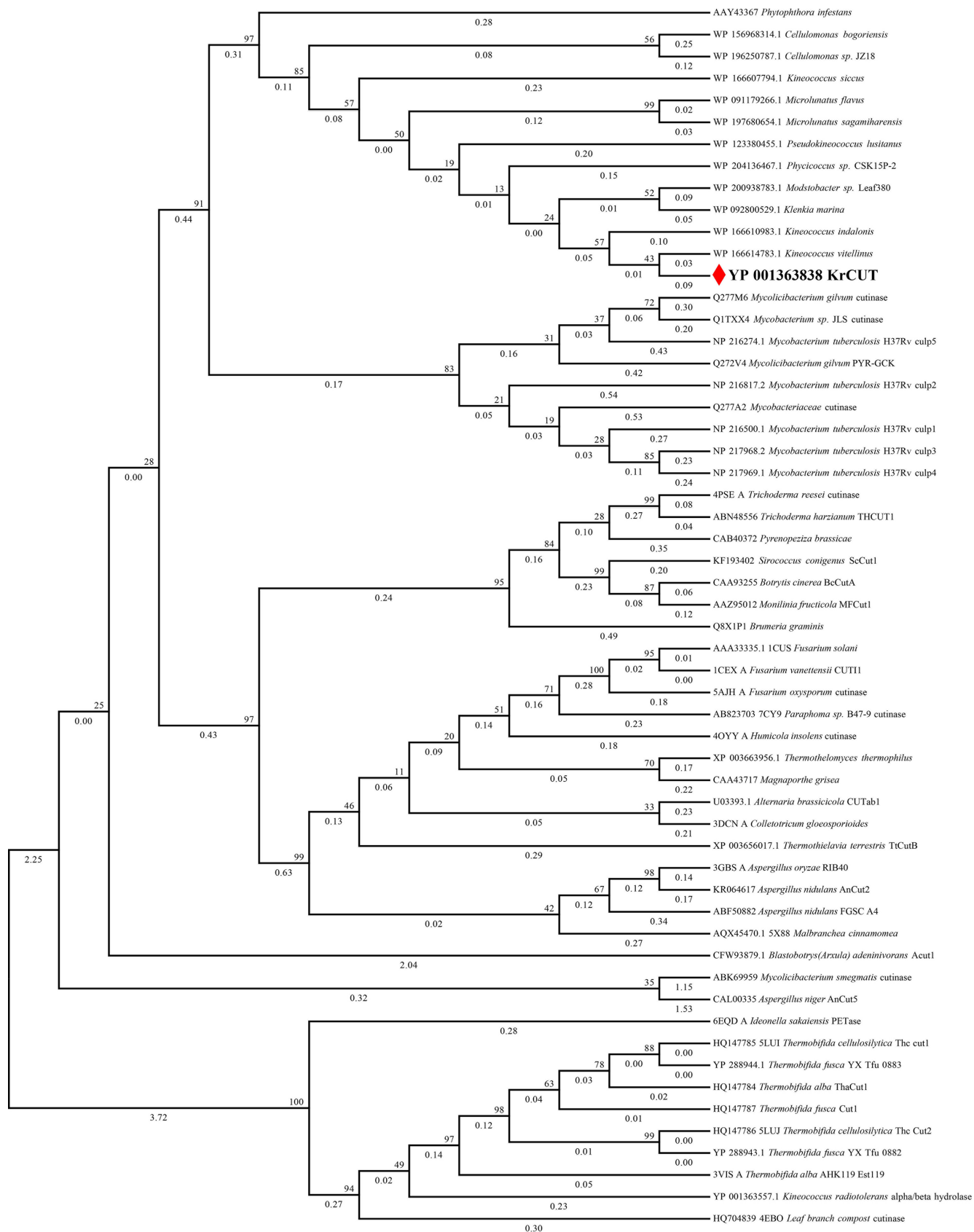


FIG 2 Phylogenetic relationship of KrCUT to other cutinases or cutinase-like sequences. The GenBank accession numbers of the sequences are as indicated preceding the organism names. Those with available crystal structures are accompanied by the Protein Data Bank (PDB) numbers. Numbers in branches indicate bootstrap values per 1,000 replicates.

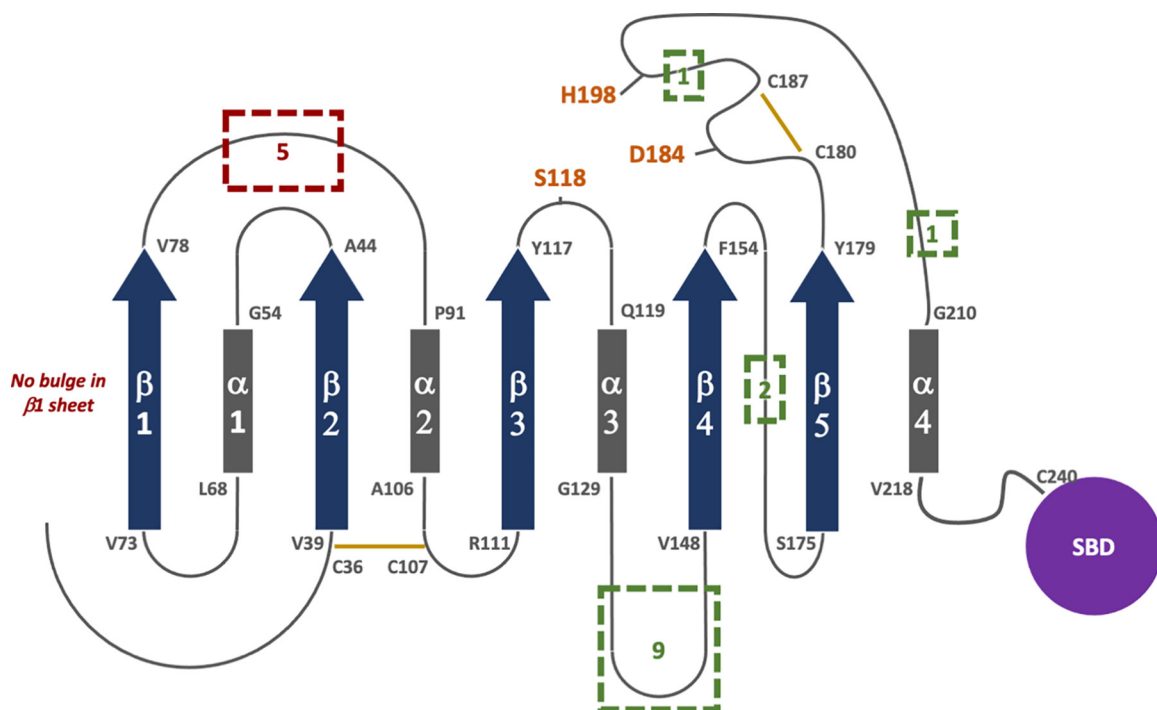


FIG 3 Secondary-structure plot of KrCUT. Identified in the dashed boxes are the locations of insertions (green) and deletions (red) compared to the *F. solani* cutinase. Orange text indicates the location of the catalytic triad, while yellow lines show locations of disulfide bonds within the catalytic domain. The substrate binding domain is shown as a cartoon sphere, as there is no structural template available with high similarity for this region.

for the original models but are still on par with the score for the crystal structures and suggest that the models are plausible.

Purification of KrCUT fusion protein and variant, enzymatic activity, and parameters.

Cutinase activity, measured using *p*-nitrophenyl (*p*NP)-butyrate as the substrate, was detected in *E. coli*(pKK233-2-YebF-KrCUT) culture after overnight induction by isopropyl- β -D-1-thiogalactopyranoside (IPTG) with activity of about 3 U/mL. Of note, the initial clone of the KrCUT-encoding gene was in the pUC57 vector provided by GenScript Corp. (Table 1 and Materials and Methods). Although a correct-sized KrCUT was produced via SDS-PAGE analysis, the protein was found in inclusion bodies and hence not further investigated but used for the subcloning in the pKK233-2 vector.

Figure 4 shows the production of the 39-kDa YebF-KrCUT fusion protein, consistent with the total molecular mass of the 10-kDa YebF carrier protein and the 29-kDa mature KrCUT. The YebF-KrCUT fusion protein was purified to electrophoretic homogeneity in two steps involving cation exchange and size exclusion chromatography (SEC). Proteins bound on SP-Sepharose eluted in two active peaks: peak 1 (minor) at a lower ionic strength and peak 2 (major) at a higher ionic strength (data not shown). The height of peak 1 eluting from the SP-Sepharose column increased over time, while peak 2 decreased in height, indicating some processing of peak 1 protein species under storage conditions (data not shown). This was confirmed by SDS-PAGE analysis of fractions from the major peak 2, which showed two protein bands of 39 kDa and 31 kDa. These two species could be separated by

TABLE 1 Oligonucleotides used for PCR amplification and cloning

Primer	Oligonucleotide sequence (5'-3')	Purpose
P1	GAGCTGCAGGCAGTTCAGTGAC	Amplification of mature portion of KrCUT (P1 and P2)
P2	GCAGAAAGCTTCAACAAGCAGTTACCAAG	
P3	TGTAAAGCTTCAATGGTAGGAACCGCGT	Amplification of KrCUT206 (P1 and P3)
P4	CGAGGAATTCAATGGAGAAAAACATGAAAAAAAG	Amplification of <i>yebF</i> (P4 and P5)
P5	GAACTGCAGACGCCGCTGATATTCCGC	

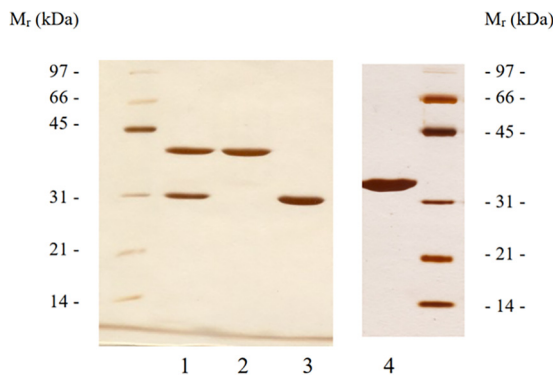


FIG 4 Purification of recombinant *K. radiotolerans* cutinase and truncated derivatives. Proteins were analyzed by 10% SDS-PAGE and silver stained. The molecular weight markers are indicated on the sides of the gels. Lane 1, fraction from SP-Sepharose showing YebF-KrCUT fusion protein (39 kDa) and mature KrCUT (31 kDa); lanes 2 and 3, fractions from HiLoad Superdex 75 showing the separated protein bands; lane 4, YebF-KrCUT206 (33 kDa) from HiLoad Superdex 75.

an additional SEC step (Fig. 4). N-terminal amino acid sequencing helped to establish the identity of the protein bands. The sequence ANNTEKSVT derived from the 39-kDa protein band corresponds to the first 10 amino acids of the mature portion of YebF, confirming a previous finding that the carrier protein is cleaved immediately after the 21-amino-acid secretory leader sequence (34). The N-terminal amino acid sequence (AT[A]SDVDVVF) of the 31-kDa species is identical to the first 10 amino acids of the mature cutinase except for a disparate Ala in the third position versus Cys in the DNA-predicted sequence (Fig. 1B), which can be explained by the fact that Cys without chemical modification is not detectable by Edman degradation.

When the protein was purified immediately after fermentation, it exclusively yielded the intact YebF-KrCUT fusion protein. However, upon storage for several weeks at 4°C, the fusion protein band underwent processing to produce a 31-kDa species that represents the mature cutinase.

The truncated KrCUT206 protein devoid of the C-terminal 55 amino acids was purified in a similar way as YebF-KrCUT as described above (Fig. 4), and its activity toward several *p*-NP esters was compared to that of KrCUT (Fig. S4). With KrCUT, the highest activity was obtained with *p*NP-butyratate (800 U/mg), with an 8-fold-higher activity over *p*NP-palmitate. KrCUT206 generally gave lower activity with various substrates than the full-length protein, although its highest activity was toward *p*NP-myristate. In both cases, *p*NB-acetate was a poor substrate.

The pH dependence of both KrCUT and KrCUT206 was analyzed at pH values ranging from 5 to 10, and the maximal activity using *p*NB-butyratate as the substrate was found at pH 8 for both (Fig. S5).

Circular-dichroism study. Both KrCUT and KrCUT206 showed the typical α -helical protein circular-dichroism (CD) spectrum with negative bands at 210 and 222 nm, although a slight difference at the 210-nm region was observed between the two proteins (Fig. 5A). An assessment of thermal stability of the two proteins, monitored at 222 nm, revealed similar thermal melting temperatures (T_m), 50°C and 51°C for KrCUT206 and KrCUT, respectively (Fig. 5B).

Protein unfolding of KrCUT started at about 40°C, which is in good agreement with the estimated temperature optimum of 45°C. Interestingly, heating of both enzymes to up to 80°C showed a near complete reversibility of the unfolding process. This was confirmed by the calculation of the thermodynamic parameters (ΔH [change in enthalpy from reactants to products] and ΔS [change in entropy from reactions to products]) of the transition range (Table S3). Even after heating up to 100°C, KrCUT and KrCUT206 recovered activity to some extent, which was consistent with secondary structure observed in the CD spectra and confirmed by measuring enzymatic activity (Fig. S6). Repeated heating of the same samples (20 to 80°C) and cooling (20°C) confirmed the reversibility of the unfolding process,

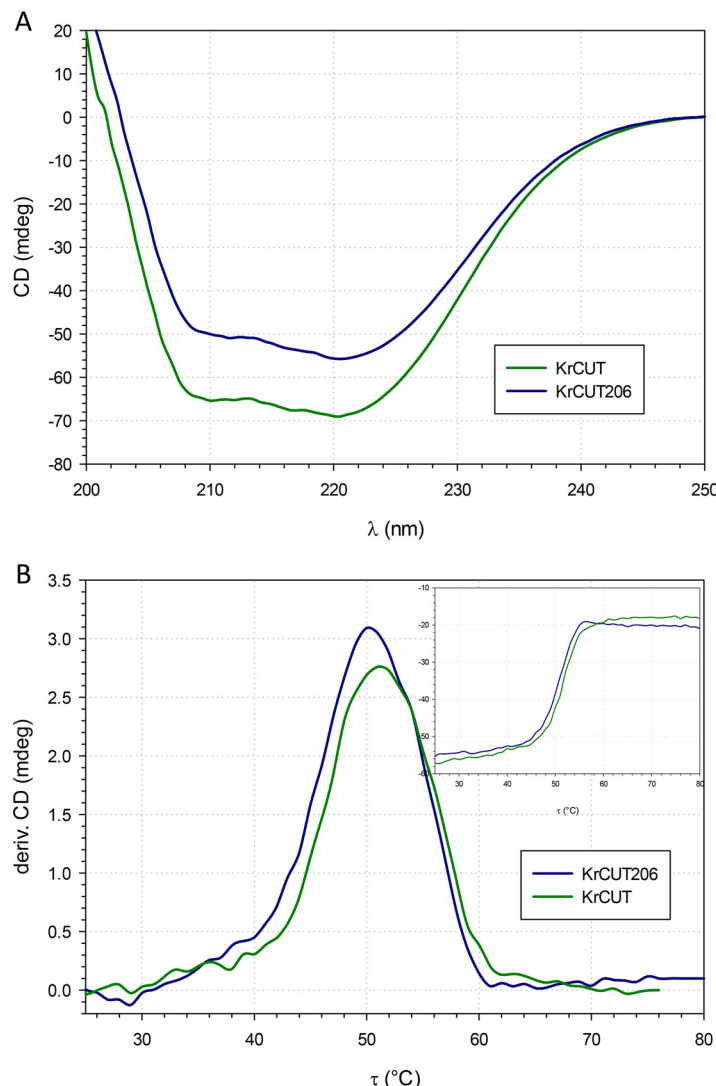


FIG 5 CD spectra of KrCUT and KrCUT206 (A) and thermal denaturation curves (B) at 222 nm. CD derivatives were calculated using Spectra Manager (Jasco). The inset shows the original thermodenaturation curves of the two proteins, measured at 222 nm while increasing the temperature.

showing a shift of the thermal transition midpoint T_m ($\Delta G = 0$) for the protein refolding to about 35°C (Fig. S7).

Hydrolysis of cutin. Assays of cutin hydrolysis were performed at two different enzyme concentrations. Characteristic cutin components, C₁₆ and C₁₈ hydroxyl fatty acids, were identified by gas chromatography-mass spectrometry (GC-MS) analysis (data not shown). 18-Hydroxy-octadeca-9,12-dienoic acid, 10,16-dihydroxyhexadecanoic acid, and 9,10,18-trihydroxyoctadecanoic acid, with retention times of 55.13, 55.92, and 64.20, respectively, were found to be the major products of hydrolysis (Table 1). Additional components of C₁₆ and C₁₈ fatty acids were identified as 9,16-dihydroxyhexadecanoic acid (55.24 min), 9,10,18-trihydroxyoctadec-10,12-dienoic acid (63.37 min), and 9,10,18-trihydroxyoctadec-9-enoic acid (66.19 min).

Degradation of synthetic polyesters by YebF-KrCUT and KrCUT206. An initial plate clearing assay indicated that a lawn of *E. coli* JM109 cells harboring YebF-KrCUT could produce a large clearing zone with polycaprolactone (PCL) as the substrate (data not shown). To quantify this further, pellets of PCL as well as films of PCL were incubated with YebF-KrCUT at various enzyme concentrations (1.25 μM, 2.5 μM, and 5 μM representing 4.7, 9.5, and 19 enzyme units) at 37°C. The degradation of the polymer was followed over

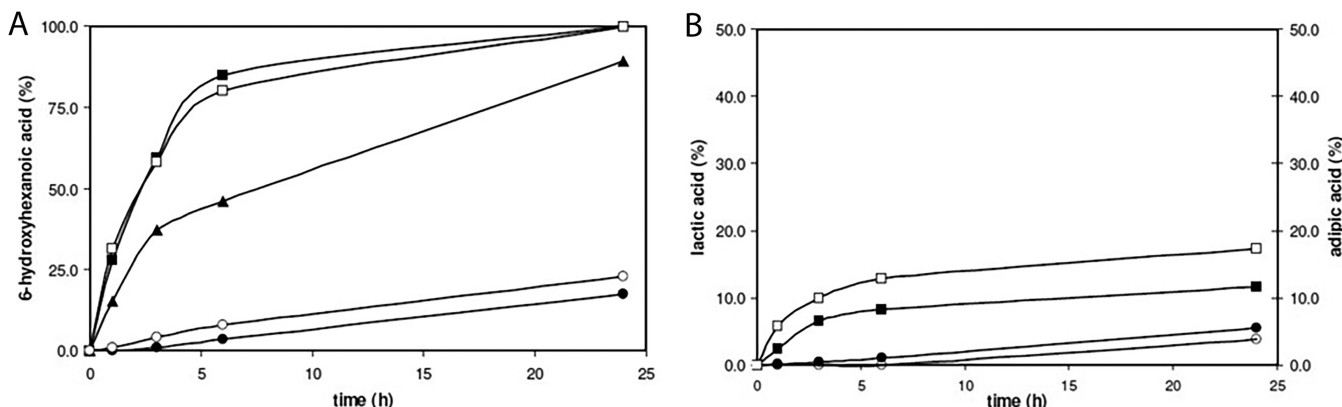


FIG 6 Degradation of synthetic polyesters by YebF-KrCUT and KrCUT206. Enzyme concentration is 2.5 μM , unless otherwise stated. (A) Degradation of PCL films (■, YebF-KrCUT; ▲, YebF-KrCUT, 1.25 μM ; □, KrCUT206) and PCL pellets (●, YebF-KrCUT; ○, KrCUT206). The curve of PCL film degradation by 5 μM YebF-KrCUT was found to approximate that of 2.5 μM enzyme concentration (data not shown). (B) Degradation of PLA (●, YebF-KrCUT; ○, KrCUT206) and polypropylene adipate (■, YebF-KrCUT; □, KrCUT206).

time by analyzing aliquots of the reaction mixture by high-performance liquid chromatography (HPLC) for the detection of the released monomer (6-hydroxyhexanoic acid) and characterization of the remaining polymer by SEC after lyophilization of the sample. YebF-KrCUT was able to release nearly 90% of the acidic monomers with an enzyme concentration of either 2.5 or 5 μM in 6 h. Even at a very low enzyme concentration (1.25 μM), thin films of PCL were degraded almost completely after 24 h (Fig. 6A).

Size exclusion chromatographic determination of polymer molar masses are consistent with the results obtained by HPLC. Comparison of the peak area corresponding to that of the polymer showed a gradual decrease over time, with complete disappearance of the polymer in experiments conducted with 2.5 to 5 μM after 24 h. This correlated well with the increase in acid detected (Table 2). A dramatic increase in M_n and M_w from 44,000 and 63,300 to 69,500 and 74,000 (Table 3) emphasized the preference of YebF-KrCUT for low-molecular-weight polymers. The degradation of PCL pellets proceeded more slowly, with 18% of the maximum yield of 6-hydroxyhexanoic acid detected in the reaction mixture after incubation with 2.5 μM protein for 24 h (Fig. 6A). Presumably, the decrease in depolymerization was due to the limited surface area of the PCL pellets compared to the films. Nearly identical results were obtained when PCL pellets and PCL films were incubated with KrCUT206 (2.5 μM) (Fig. 6A).

Both YebF-KrCUT and KrCUT206 (2.5 μM ; 2 U) degraded only approximately 5% of poly-lactic acid (PLA) (Fig. 6B). However, in the case of poly(1,3-propylene adipate), a polymer consisting of alternating diacid and diol subunits, 12% and 17% of adipic acid were found in the reaction mixture containing YebF-KrCUT and KrCUT206, respectively, after 24 h (Fig. 6B). All in all, it appeared that both enzymes exhibited a preference for longer-chain monomers such as 6-hydroxyhexanoic acid and adipic acid (both C₆ unit in polymer) compared to lactic acid, a C₃ monomer.

Polymer-binding domain of KrCUT. Different polymers (cellulose, PLA, PCL, and PHB) were tested to evaluate the ability of KrCUT and truncated KrCUT206 to bind these materials. Binding assays for PCL and PLA could not be performed since both polymers were degraded by the enzymes. KrCUT did not bind to cellulose, indicating that the binding domain of the cutinase is distinct from a cellulose binding domain, as implicated by the sequence. On the other hand, KrCUT was found to bind efficiently to PHB, a reflection of the sequence similarity of this region to the binding domain of PHB depolymerases. KrCUT did not degrade PHB, consistent with the differences in sequence between the catalytic domains of cutinases and PHB depolymerases. The KrCUT206 variant showed no binding to PHB, indicating the essentiality of the C-terminal extension for this activity.

The kinetics of KrCUT adsorption to PHB is shown in Fig. 7. The curve shows the relation between the adsorbed cutinase and the equilibrium concentration of the enzyme, with the adsorption to the PHB surface expressed by the Langmuir adsorption equation. As a result, the maximum amount of cutinase adsorbed on the PHB granules (E_{\max}) was determined to

TABLE 2 Monomeric products released from apple cutin by cloned KrCUT^a

Retention time (min)	Cutin hydrolysis product	Area (20 U) (%)	Area (200 U) (%)
55.13	18-Hydroxy-octadeca-9,12-dienoic acid	18.0 ± 6.3	2.22 ± 0.13
55.24	9,16-Dihydroxyhexadecanoic acid	ND	3.81 ± 0.62
55.92	10,16-Dihydroxyhexadecanoic acid	39.3 ± 2.5	27.74 ± 0.41
63.37	9,10,18-Trihydroxyoctadec-10,12-dienoic acid	ND	13.25 ± 0.40
64.20	9,10,18-Trihydroxyoctadecanoic acid	ND	25.55 ± 0.10
66.19	9,10,18-Trihydroxyoctadec-9-enoic acid	ND	6.25 ± 0.40

^aHydrolysis was carried out at two different units of activity of cutinase. Standard deviations of triplicate measurements are shown. ND, not detected.

be $23.68 \pm 0.03 \mu\text{g}/\text{mg}$, and the adsorption equilibrium constant (K) was calculated to be $0.12 \pm 0.03 \text{ mL}/\text{mg PHB}$.

Effect of KrCUT on hemp fiber. The quantity of pectin released from natural hemp fiber by KrCUT in conjunction with the action of a thermostable pectate lyase was assessed. The thermostable pectate lyase alone released a certain amount of pectin as expected of the pectinolytic activity (35). With an increasing amount of added cutinase, a higher percentage of pectin degradation products was detected when the quantity of added pectate lyase was kept constant. When KrCUT was incubated with hemp fiber at the highest concentration in the absence of pectate lyase, a negligible amount of pectin from the fiber material was detected (Fig. 8).

The effect of KrCUT on the hemp fiber integrity was visualized using light microscopy and scanning electron microscopy (SEM). Light microscopic images revealed that treatment of fibers by both cutinase and pectate lyase appeared to produce more separated fiber bundles, whereas pectate lyase alone showed more fibers embedded in pectin and wax material (Fig. S8). The SEM pictures showed that cutinase treatment gave more separated fibers having a cleaner surface than those of pectate lyase-treated samples.

DISCUSSION

The KrCUT described in this study represents the first hydrolytic enzyme of the radio-resistant actinomycete *K. radiotolerans* characterized at both the biochemical and molecular levels. Other investigations were focused on the transcriptome analysis of small noncoding RNAs that led to the prediction of some highly expressed genes, and in an isolated case a xeroderma pigmentosum type B helicase-encoding gene was characterized at the biochemical level (28, 36–39).

The modular structure of KrCUT containing a C-terminal extension with a linker is unprecedented among known cutinases (16, 18, 25). Thus far, this novel organization is seen in the genomes of other actinobacteria, such as *K. marina*, *M. sagamiharensis*, *M. flavus*, *Pseudokineococcus lusitanus*, *Modestobacter* sp. leaf 380, and various species of *Cellulomonas*, all of which remain uncharacterized. Interestingly, the modular KrCUT structure mirrors those of bacterial PHB depolymerases that are organized with a catalytic domain composed of an S-H-D catalytic triad followed by a linker region (~40 amino acids) that can be fibronectin type III, threonine rich or cadherin-like, and finally a substrate binding domain (SBD) of 40 to 60 amino acids (40).

In an early study, evolution of the cutinase gene family was found to be confined to two distantly related groups of phytopathogenic oomycetes (*Phytophthora*) and fungi, within the prokaryotes to three actinobacterial genera (*Mycobacterium*, *Kineococcus*, and a lone *Rhodococcus*), and no archaea (32). With an expanded data set, although by no means designed to be exhaustive, the maximum likelihood tree of cutinase (Fig. 2) showed

TABLE 3 Evidence of PCL degradation: comparison of SEC and HPLC analysis

Time (h)	PCL (SEC) (%)	M_n (kDa)	M_w (kDa)	Acid (HPLC) (%)
0	100	44.0	63.3	0
1	61	53.8	64.4	28
3	27	55.0	66.6	60
6	12	58.2	68.1	85
24	0.3	69.5	74.0	100

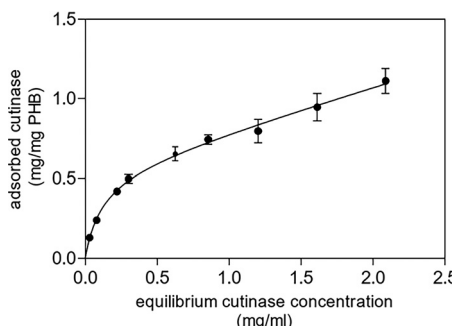


FIG 7 Adsorption isotherm of cutinase and PHB granules at 25°C. Purified KrCUT at concentrations ranging from 0.16 to 3.2 mg/mL were mixed with 25 mg PHB in 50 mM sodium phosphate (pH 8.0) in a total volume of 1 mL and mixed by gently shaking for 3 h. The PHB polymer was removed by centrifugation, and the concentration of protein in the supernatant was determined by the BCA method. The concentration of bound protein at a particular concentration of cutinase was calculated as the difference between a control without added PHB and free cutinase after incubation with PHB. P value < 0.001.

that the *Kineococcus* cluster has grown to include several other actinobacterial genera that are distinct from mycobacterial sequences and those of Ascomycetes (e.g., *Aspergillus*) as well as those from many mesophilic (e.g., *Ideonella*) and thermophilic microorganisms (Fig. 2). Inter- and intradomain gene transfers have been proposed to be important mechanisms in the evolution of the cutinase gene family (32).

The homology model (SM+LG) of KrCUT suggests a larger pocket (Fig. 9) than for FsCUT (PDB code 1CEX), similar to the pocket in AoCUT (PDB code 3GBS). This is exemplified by the larger distance between the gatekeeper residues in KrCUT ($S51_{CB}$ - $G161_{CA}$ = 9.7 Å), which is like that for AoCUT ($L87_{CB}$ - $V190_{CB}$ = 9.9 Å) but larger than for FsCUT ($L81_{CB}$ - $V184_{CB}$ = 8.7 Å). Interestingly, the identity of the gatekeeper residues in KrCUT is different, comprised of Ser51 and Gly161, while in other cutinases they are typically hydrophobic (Fig. S9). Additionally, the 5-residue deletion seen in KrCUT would normally make up one end of the pocket, but the lack of these residues opens up the pocket further, creating a larger channel than for FsCUT. While a more rigorous modeling protocol (molecular dynamics or *ab initio* loop searching) may bring the 9-residue loop insertion closer to the pocket shortening the channel, it would still remain longer than the pocket seen in FsCUT. The improved activity toward longer aliphatic chains and PCL compared to the case with FsCUT and

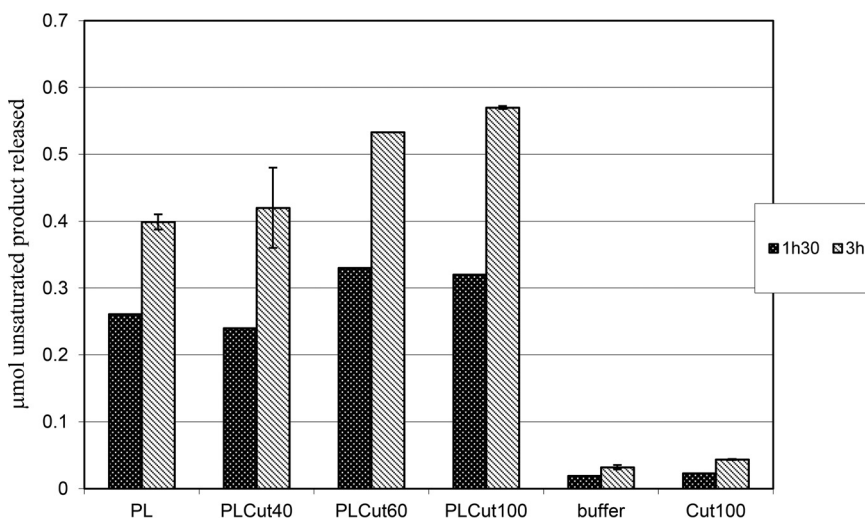


FIG 8 Amount of pectin released from natural hemp fibers by pectate lyase (PL) or in combination with cutinase (Cut) at different concentrations. The shaded bars indicate the two incubation periods. The amount of unsaturated product released is reported. PLCut40, pectate lyase and 40 units of cutinase; PLCut100, pectate lyase and 100 units of cutinase. P value = 0.024277.

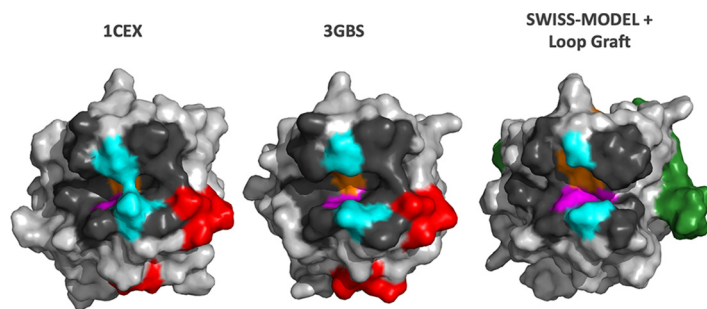


FIG 9 Pocket analysis. Pocket residues were identified by superimposing crystal structures (enabling accent secondary-structure matches refined with Gaussian weight) following alignment in MOE. Residues within 4.5 Å of the covalent ligand in *Trichoderma reesei* cutinase in complex with a C11Y4 phosphonate inhibitor (PDB code 4PSE) were assigned as pocket residues. Orange, catalytic triad; light gray, pocket residues; magenta, oxyanion hole residues; cyan, gatekeeper residues.

AoCUT may be a result of the larger pocket allowing KrCUT to better accommodate these larger substrates.

As secreted proteins, recombinant cutinases and CULPs in general have been expressed in a number of heterologous hosts, including *Saccharomyces cerevisiae*, *Aspergillus awamori*, *Bacillus subtilis*, *E. coli*, and *Pichia pastoris*, depending on the source of the enzyme (3, 16, 18, 41). Secretion in *E. coli* made use of fusion of the cutinase-encoding sequence to signal peptides, such as PelB, OmpA, and α -hemolysin, that had given various successes. We took a different approach by fusing KrCUT to the *E. coli* YebF periplasmic protein, demonstrated through the premier study of Zhang et al. (34) to readily export proteins like α -amylase, human interleukin-2, and alkaline phosphatase into the medium. Although the exact mechanism is not known, the export of YebF was subsequently shown to be porin mediated, involving OmpF, OmpC, and OmpX (42). In addition, the YebF carrier protein was predicted to be “truly secreted and released” by *in silico* studies (43). In this study, although KrCUT was successfully expressed as a fusion protein to the C-terminal end of YebF, and secreted to the medium, two observations are worth noting. First, the cutinase activity in the fused YebF-KrCUT entity was somewhat suppressed in the presence of YebF with no ready explanation. Second, the YebF carrier protein was fortuitously cleaved, rendering the desirable intact KrCUT protein. The exact basis for this *ex situ* processing is unknown except that the C terminus of YebF contains a double arginine, making the fusion junction a possible trypsin-like or other serine protease cleavage site (44). We have performed a scaled-up fermentation of KrCUT at a 10-L volume and achieved a modest KrCUT concentration of 220 mg/L, corresponding to an enzyme activity of 1,425 U/L, using *p*NP-palmitate as the substrate. One of the highest extracellular cutinase activities reported in the literature is that of *T. fusca* Tfu_0883 produced in *E. coli* BL21(DE3), with values of 5.1 g/L, corresponding to 2258.5 U/mL when measured with *p*NP-butrate as the substrate (45). Using a *P. pastoris* system, Duan et al. (46) reported a yield of 12,535 U/mL of a thermophilic cutinase from *Malbranchea cinnamomea* in a 5-L fermentor.

The catalytic domain of KrCUT comprising of 261 amino acids with an M_r of 31 kDa is consistent with the molecular masses of the majority of bacterial cutinases, although those of fungal origin are generally smaller (16, 18). The pH optimum at 8 of KrCUT falls in the range of 7.0 to 9.5 for a great number of cutinases (16). At 45°C, the thermostability of KrCUT is not as high as those of bacterial cutinases that are derived from thermophilic actinomycetes, whose optimal temperatures are in the range of 50 to 60°C. Nonetheless, it is remarkable that thermal unfolding of KrCUT as well as its truncated variant upon heating to 80°C resulted in complete reversibility after cooling. Various factors, including secondary structure content and composition within domains and interaction or conformation of domains may contribute to the reversible folding of an enzyme. Among other hydrophobic or polar interactions, the disulfide bond is one of the stabilizing factors of the proteins. KrCUT has six cysteines, two pairs of which, C3-C74 and C148-155, correspond to the disulfide bridges C31-C109 and C171-C178, respectively, of the prototypical FsCUT, which have

been shown to confer stabilization of the global molecular folding and maintenance of structural integrity of the active site (47, 48). The number of disulfide bonds in published cutinase structures varies from one to three (references 18, 49, and 50 and references therein). For instance, the single disulfide bond (C275-C292) in LCC was found to contribute to both thermodynamic and kinetic stability of the enzyme (15). AoCUT has three disulfide bonds (20), two of which are well conserved among other cutinase structures. However, the number of disulfide bridges does not translate to added thermostability when cutinase of *M. cinnamomea* (McCUT) with two S-S bonds was found to display much higher thermostability than AoCUT and most cutinases (46). Like KrCUT, McCUT displayed maximal activity at 45°C, but it retained more than 85% of its initial activity after incubation at 75°C for 30 min.

The two additional Cys residues in KrCUT are found at either end of the 55-amino-acid C-terminal extension, both being invariant among the substrate binding domains of PHB depolymerases (Fig. 1). That there are no free sulphydryl groups in KrCUT according to *para*-chloromercuribenzoate assay at concentrations of 0.01 to 1 mM (results not shown) would suggest that all the Cys in KrCUT are involved in disulfide bonding. This remains to be confirmed by structural work, which was outside the scope of the present study. At any rate, thermal reversibility of KrCUT may be an attribute to the functionality of the protein in various applications, although it may not be suitable for polyethylene terephthalate (PET) hydrolysis since it requires a temperature close to the glass transition temperature of PET, i.e., 60 to 70°C in water (51). Incidentally, a putative α/β fold hydrolase of *Kineococcus* is found to cluster with a number of PET-degrading enzymes (Fig. 2). In the future, it will be interesting to explore the potential of this gene candidate for plastic recycling.

We demonstrated that KrCUT206 lacking the C-terminal 55 amino acids was unable to bind PHB, unlike the full-length protein. The kinetics of adsorption of KrCUT to PHB granules appeared to obey the Langmuir isotherm. The experimentally determined E_{\max} value of about 24 mg/ μ g polyester material is in the range of 19 to 31 mg/ μ g toward poly(3-hydroxybutyrate) or poly(2-hydroxypropionate), established for PHB depolymerases from *Alcaligenes faecalis* (*PhaZ_{Afa}*), *Comamonas acidovorans* (*PhaZ_{Cac}*), and *Comamonas testosteroni* (*PhaZ_{Cte}*) (52). We had not determined the diameters of the PHB granules by scanning electron microscopy, for example, to get an estimate of a cross-area per molecule of KrCUT bound to the surface of PHB granules. However, heterogeneity of the polymer particle size most likely will affect this type of calculation. To fully investigate the binding/association and dissociation phases or behavior of KrCUT adsorption to PHB, surface plasmon resonance technology will be required.

Several conserved amino acids in the type 1 SBD of various PHB depolymerases (30, 31, 40) and the putative substrate or polymer-binding domain of KrCUT (Fig. 1) may be factors contributing to the hydrophobic interactions between the hydrophobic residues in the enzyme and the methyl groups in the polymer and also the hydrogen bonding between the hydrophilic residues in the enzyme and the ester bonds in the polymer (30). Whereas in PHB depolymerases the SBD is responsible for the adsorption of the enzyme to the polymer surface, thus permitting an efficient hydrolysis by the catalytic domain, the exact role of this C-terminal extension in KrCUT appears to be an enigma. Considering the harsh and highly mutagenic environment that the organism was exposed to, it is conceivable that lateral gene transfer among the high-G+C and Gram-positive bacteria followed by domain shuffling would result in potential loss or gain of a particular attribute. Interestingly, the Pro-Thr linker in KrCUT was found to be most similar in composition and length to that of the modular xylanase (Cex) from *Cellulomonas fimi*, where a 20-residue linker with the sequence (PT)3T(PT)3T(PT)3 functions as a flexible tether joining the structurally independent catalytic and cellulose binding domains as "two beads on a string" (reference 53 and references therein). In addition, the PT linker was previously found to be O-glycosylated, a modification that confers resistance against proteolytic degradation.

Aside from having the characteristics of a high C_4/C_{16} ratio of activity toward *p*NP-butyr ate and *p*NP-palmitate that typifies a number of microbial cutinases (46, 54, 55), the cutinase activity of KrCUT was further established by the identification of representative cutin monomers, C_{16} and C_{18} hydroxyl fatty acids, in the mass chromatograms of the enzymatic reaction

containing apple cutin as the substrate (56). Furthermore, both YebF-KrCUT and KrCUT206 were shown to be rather efficient biocatalysts for the degradation of synthetic polyesters, the hydrolysis of polyester PCL being correlated with KrCUT activity as in the prototypical FsCUT (57) and other related studies (16). Both KrCUT and KrCUT206 showed excellent activity toward aliphatic polyesters consisting of C₆ acids, and those made up of smaller acid units such as PLA and PHB were degraded significantly slower or not at all. Compared to the depolymerization of PCL films by FsCUT or AoCUT from *A. oryzae* (20), the KrCUT enzyme and truncated variant appeared to have an edge. With AoCUT, an enzyme concentration of 8.8 μM led to 87% degradation of 12- to 14-mg/mL PCL films in 6 h, whereas a 2.5 μM concentration of either YebF-KrCUT or KrCUT206 could degrade 80 to 85% of 10-mg/mL PCL in the same time frame. In a comparative study of five cutinases, FsCUT was found to function poorly for the degradation of PCL in terms of stability and at high temperatures as well as under acid pH conditions (58). Shi et al. (59) showed that a *Candida* lipase was more suitable for the degradation of PCL films than FsCUT at the same enzyme concentrations. In general, members of actinobacteria are found to play an important role in PLA degradation (60).

The notion of using cutinase (commercially available *Pseudomonas* cutinase) in the bioscouring of cotton fiber cuticle was exploited back in 2002, resulting in an improvement in wettability of raw cotton fabrics (61). Moreover, together with a pectin lyase (Pectazym HF), a synergistic effect between the two enzymes in increasing water absorbency of the cotton fabrics was reported. The rationale for this is that specific degradation of the cuticle would lead to an increase in pectinase action on the pectin backbone. The synergistic effect of the two commercially available enzymes on the hydrolysis of cotton fiber cuticle was revisited by Degani recently (62), including an assessment of increased fabric weight loss and wax removal. Related studies by Agrawal et al. (63, 64) demonstrated a low-temperature (25 to 30°C) cotton wax removal by FsCUT, a pretreatment that led to a reduced bioscouring time by BioPrep3000L, a commercially available pectate lyase.

For the first time, a cutinase was applied to a natural bast fiber, and we have demonstrated a similar synergistic effect with an engineered pectate lyase of added thermostability (35) on the degradation of pectin prepared from hemp fiber. Preliminary SEM pictures showed better-separated fiber bundles, if not cleaner surfaces, than those for fibers treated with pectate lyase alone. Scaling up of the pectate lyase-cutinase alkaline cocktail for the possible preparation of higher-quality hemp or flax fibers is a challenging endeavor for a sustainable future. The fact that KrCUT is not inhibited by EDTA (results not shown) means that it is compatible in a cocktail mix that includes pectate lyase and EDTA, a combination found previously to be most effective for the retting of flax (65).

Nonetheless, the discovery and characterization of a prototype naturally occurring modular cutinase paves the way for stimulating and fostering new research findings in areas that go beyond the hydrolytic power and the conventional list of applications. From a structure-function viewpoint, evidently there is still much to learn, particularly regarding the C-terminal domain, for which there are no structural data. As a secreted protein, cutinase has the potential of being developed as a subunit vaccine antigen (66, 67). This study also reiterates the need to characterize new microorganisms in the environment, not only because we want to enrich the little that we know about microbial diversity but also because new microorganisms may have interesting new metabolic or biocatalytic properties (68).

MATERIALS AND METHODS

Reagents and chemicals. *p*-Nitrophenyl (*p*NP) esters were purchased from Fluka (Steinheim, Germany) or from Sigma-Aldrich (USA). Lactic acid, 6-hydroxyhexanoic acid, adipic acid, polycaprolactone (PCL; M_n = 42,500; M_w = 65,000), poly(lactic acid) (PLA; M_n = 30,000; M_w = 60,000), poly(1,3-propylene adipate) (PPA; M_n = 42,500; M_w = 4,800), and poly(R)-3-hydroxybutyrate (PHB) were purchased from Sigma-Aldrich, Fluka, or Alfa Aesar (Ward Hill, MA). Restriction endonucleases were purchased from New England BioLabs (Pickering, ON, Canada), T4 DNA ligase was from Roche (Mannheim, Germany) and Titanium DNA polymerase from Clontech (TaKaRa Bio, USA).

Genome mining and cloning of cutinase-encoding gene and variants. The 885-bp Krad_4111 locus tag of the *K. radiotolerans* genome (YP_001363838.1 [29]), encoding a potential cutinase gene, was chosen as the result of a BLAST search using the amino acid sequence of FsCUT as a query sequence.

The gene was initially cloned into a recombinant pUC57 plasmid (GenScript Corporation, Piscataway, NJ) as a synthetic construct after codon optimization (reducing the G+C content from 77.2% to 59%) for expression in *E. coli*. Subclones were then made in the IPTG-inducible vector pKK223-2 with primer set P1 and P2 (Table 1), designed to amplify the mature portion of the KrCUT-encoding gene (codons 34 to 294), and P1 and P3 (Table 1), to amplify a truncated KrCUT206 (codons 34 to 220) lacking the C-terminal 74 amino acids. Each primer set contains a 5' PstI site and 3' HindIII site for directional cloning. The PCR parameters were 94°C 3 min, 30 cycles of 94°C for 45 s, $T_m - 3^\circ\text{C}$ for 30 s, and 68°C for 1 min, followed by a final extension at 68°C for 10 min.

To express KrCUT and its variant in a secreted form, the *E. coli* extracellular carrier protein YebF (34) was used to construct N-terminal fusion proteins. The sequence encoding YebF 366-bp without the stop codon but including the signal peptide (NCBI B1847) was amplified by primers P4 and P5 containing the EcoRI and PstI restriction sites (Table 1). The PCR fragment was gel purified and cloned upstream of the KrCUT-encoding gene in pKK223-2 to produce pKK223-2-YebF-KrCUT and pKK223-2-YebF-KrCUT206. These recombinant plasmids were transformed into *E. coli* JM109 cells by conventional techniques (69). The cloned genes were verified by DNA sequencing using a BigDye DNA sequencing kit (Applied Biosystems) and an automated DNA sequencer (model 377 ABI Prism).

Protein expression. A single colony of *E. coli* JM109 cells harboring either YebF-KrCUT or YebF-KrCUT206 was grown at 30°C on a rotary shaker at 200 rpm in 10 mL Terrific broth (TB) medium supplemented with 100 µg/mL ampicillin. The overnight culture was used to inoculate 1 L fresh TB medium and then grown to an optical density at 600 nm (OD_{600}) of 0.4 to 0.5 under the same culture conditions and induced with 0.1 mM IPTG for 16 h. The cells were collected by centrifugation at 5,000 × *g* for 30 min (Beckman centrifuge, model J2-21M), and the supernatant was used as a source of cutinase. Protein concentration was determined using the bicinchoninic acid (BCA) method (70).

Fermentation in DASGIP system. A single colony of *E. coli* JM109 cells harboring either YebF-KrCUT or YebF-KrCUT206 was cultured in LB medium containing ampicillin (0.1 g/L) and incubated at 30°C in a rotary shaker at 200 rpm overnight. The preculture (5% [vol/vol] of the total fermentation volume) was added to TB medium (1 L) in a 2-L fermentor (DASGIP, Germany). The temperature was set to 30°C, and the pH was controlled at 7.0 by the addition of concentrated ammonium hydroxide. The cell broth was aerated at 1.0 volume of airflow per volume of liquid per minute (vvm) and stirred at 400 to 900 rpm to maintain 30% dissolved oxygen. If necessary, the airflow was supplemented with oxygen. At an OD_{600} of 9 (~7 h), cutinase expression was induced by the addition of IPTG (final concentration, 1 mM); the temperature was set to 25°C, and glucose (33% [wt/wt] aqueous solution) was fed at an initial rate of 3 mL/h and gradually increased to 6 mL/h. The cells were harvested after 16 h, and centrifugation of the cell broth (5,000 × *g*, 4°C, 20 min) yielded 0.82 to 0.87 L of supernatant that was used to purify the corresponding cutinase.

Protein purification. All purification procedures were performed at 4°C on an ÄKTAexplorer 100 Air chromatography system (GE Healthcare). Culture supernatant containing active enzyme was concentrated and dialyzed against sodium phosphate buffer (20 mM, pH 7.0) by cross flow filtration using the QuixStand system (GE Healthcare) equipped with a hollow-fiber cartridge (3-kDa cutoff). The enzyme solution was loaded onto a SP-Sepharose FF column (XK 50/12) previously equilibrated with 20 mM sodium phosphate buffer (pH 6.0). The flow rate was 4.0 mL/min. The column was washed with the same buffer until no protein could be detected in the flowthrough, and the enzyme was subsequently eluted with a linear gradient of 0 to 0.6 M NaCl. Active fractions were pooled and concentrated by ultrafiltration (membrane exclusion size, 10 kDa) in a 100-mL stirring cell (Amicon, USA) and then applied to a HiLoad Superdex 75 prep grade (16/60) column previously equilibrated with 20 mM sodium phosphate buffer (pH 7.0) containing 150 mM NaCl. Protein was eluted with the same buffer at a flow rate of 1.5 mL/min and collected in 2-mL fractions. The protein profile was monitored by its absorbance at 280 nm.

Protein sequencing. Purified enzymes were separated by SDS-PAGE (10%) and transferred onto a polyvinylidene difluoride membrane (Bio-Rad, USA). N-terminal sequencing was carried out by the Sheldon Biotechnology Centre (McGill University, Montreal, Canada). Phenylthiohydantoin amino acids were analyzed by HPLC using a reversed-phase column.

Esterase assay. Esterase activity was determined by monitoring the formation of *p*NP at 410 nm from various *p*NP esters using a Beckman UV spectrophotometer (model DU 640). Substrates were dissolved in isopropanol and were added to 50 mM sodium phosphate buffer (pH 8.0) to give a 10% (vol/vol) total isopropanol concentration in a 1-mL reaction volume. *p*NP-butyrate was used as a final concentration of 1.2 mM. For *p*NP-caprylate, -myristate, and -palmitate, the final concentration ranged from 0.1 to 0.5 mM. The reaction (1 mL) was started by adding an appropriate amount of enzyme. One enzyme unit is defined as the amount of enzyme that produced 1 µmol product (*p*NP) per min; specific activity is expressed as units per milligram protein. A molar extinction coefficient of 15 mM⁻¹ cm⁻¹ for *p*NP was used for calculating enzyme activity.

CD spectroscopy. Circular-dichroism (CD) spectra were recorded using a Jasco J-815 spectrometer operating with the Spectra Manager software. Temperature was controlled using a Jasco PFD-452S Peltier unit. Active protein (KrCUT and KrCUT206) was desalting using a HiPrep desalting column (26/10) previously equilibrated with 20 mM sodium phosphate buffer (pH 7.0). The final protein concentration was adjusted to 0.15 mg/mL (~6 µM), and CD spectra were recorded between 190 and 250 nm using a quartz cuvette (inside diameter [i.d.] = 0.1 cm). Blanks containing buffer only were prepared and used as baseline. Temperature-dependent protein unfolding was monitored at 222 nm with thermal profiles ranging from 20 to 100°C (2°C min⁻¹). Samples were kept for 5 min at the respective maximum temperature, and protein refolding was monitored using the same conditions as described above, reversing the thermal profiles. Thermodynamic parameters (T_m , ΔH , ΔS , and ΔG) for the folding/unfolding process were calculated using the Spectra Manager software.

Adsorption assays. PHB granules were prepared and purified according to the method of Kasuya et al. by dissolving the polymer in chloroform and precipitated by addition of methanol (52). Adsorption

assays were also carried out following the procedures of Kasuya et al. (52). Purified KrCUT and truncated KrCUT206 at concentrations ranging from 0.16 to 3.2 mg/mL were added to a suspension of 25 mg PHB in 50 mM sodium phosphate (pH 8.0) in a total volume of 1 mL. The mixture was incubated at room temperature with gentle shaking for at least 3 h. The PHB polymer was removed by centrifugation, and the concentration of protein in the supernatant was determined by the BCA method. The concentration of bound protein at a particular concentration of cutinase was calculated as the difference between a control without added PHB and free cutinase after incubation with PHB. An isotherm of [bound] (milligram per milligram PHB) versus [free] (millimolar) was generated, and binding parameters were determined by nonlinear regression using the Langmuir equation:

$$E_{ad} = E_{\max} \left(\frac{K[E]e}{1+K[E]e} \right)$$

where $[E] = E_{ad} + [E]e$ (E_{ad} being the amount of protein adsorbed on the surface of polymer granules and $[E]e$ being equilibrium concentration of protein) and is the concentration of the protein added, E_{\max} is the maximum amount of protein adsorbed on the polyester granules, and K is the adsorption equilibrium constant of the protein.

Phylogenetic analysis. The maximum likelihood method based on the Whelan and Goldman model (71) was used. Evolutionary analyses were conducted in MEGA7 (72).

Computational models. The SWISS-MODEL web server was used to build a homology model (33). Details are provided in supplemental method i in the supplemental material.

Cutin preparation and monomer analysis. Cutin preparation from the outer layer of a Golden Delicious apple was carried out essentially as described by Gerard et al. (56). Details can be found in supplemental method ii as well as the procedures for the derivation of cutin monomers and component analysis.

Degradation of polyesters and analysis. An appropriate amount of cutinase was added to a 20-mg quantity of the polymer to be analyzed (PCL, PLA, PHB, or PPA) in 50 mM phosphate buffer (pH 8). The reaction mixture (2 mL) was shaken at 37°C at 175 rpm on an orbital shaker. Samples were taken after 1, 3, 6, and 24 h, and aliquots of 50 μL were analyzed by HPLC (see supplemental method iii); the remaining mixtures were frozen and subsequently lyophilized. The resulting solid (~40 to 50 mg) was dissolved in tetrahydrofuran, filtered, diluted (1.5 to 2 mg/mL), and analyzed by SEC (see supplemental method iv).

Alternatively, a thin film was prepared from 1 g commercially available PCL pellets and used for degradation. The polymer was dissolved in dichloromethane in a 1-L beaker. The solvent was allowed to evaporate overnight, and the resulting film was dried to constant weight under reduced pressure. Prior to enzymatic treatment, the film was cut into pieces (20 mg) of approximately 1.5 cm by 1.5 cm and a thickness of approximately 0.1 mm. The reaction mixture was monitored by HPLC and SEC as indicated above.

Enzymatic activity on hemp fibers. Hemp fibers (German variety) were purchased from Biolin Research Inc. Fibers (150 mg) were treated with either pectate lyase (PL; 10 U) or PL combined with various amounts of KrCUT (40, 60, and 100 U). The source of PL was as described by Xiao et al. (35). Control experiments containing no enzyme or 100 U of KrCUT were conducted for comparison. After incubation at 37°C, aliquots of the reaction mixture were taken at 1 h 30 min and 3 h and analyzed for pectin degradation products using the thiobarbituric acid (TBA) method (73), which detects released unsaturated compounds spectrophotometrically at 550 nm.

For microscopy analysis, hemp fibers were prepared as follows. Hemp stems (50 cm, 25 g) were treated with KrCUT (100 U/g) together with PL (20 U/g). The reaction was carried out in 50 mM Tris-HCl (pH 8.0) supplemented with 0.5 mM CaCl₂ (required for PL). The samples were incubated at 37°C with gentle shaking at 100 rpm for 16 h. The stems were removed from the enzymatic solution and peeled off by hand, and the resulting fiber was washed with hot water to inactivate the enzymes. After removal of the outer layer debris by rinsing with cold water, the fibers were air dried. A sample of the hemp stem treated only with PL was prepared for comparison. These experiments were conducted in duplicate. The dried fibers were spread onto a microscope slide and observed by light microscopy. A scanning electron microscopy (SEM) analysis was also conducted using a Hitachi S-4700 at a voltage of 2 kV to observe the fiber surface and fiber bundle.

Data availability. The Krad_4111 locus tag of the *K. radiotolerans* genome, YP_001363838.1, is gene complement 1986432 to 1987316 of GenBank accession number CP000750.2 (Protein ID ABS05574.1).

SUPPLEMENTAL MATERIAL

Supplemental material is available online only.

SUPPLEMENTAL FILE 1, PDF file, 1.2 MB.

ACKNOWLEDGMENTS

This research was initiated through the support of the Climate Change Technology and Innovation Biotechnology Program of the Canadian Biomass Innovation Network of Natural Resources Canada.

We thank L. Shimkets for supplying the *Kineococcus* strain and J. Weiner for the secretion vector. We are grateful to H. Bergeron, A. Corriveau, S. Deschamps, and L. Paquet for their expert technical help, Jiaqi Duan and Guangyue Li for help with the phylogenetic tree, J. Denault for her collaboration, and A. Matte for suggestions and help with the manuscript.

REFERENCES

- Riederer M, Mueller C. 2006. Annual plant reviews, vol 23. Biology of the plant cuticle. Blackwell Publishing Ltd, Oxford, United Kingdom.
- Kolattukudy PE. 2001. Polyesters in higher plants. *Adv Biochem Eng Biotechnol* 71:1–49. https://doi.org/10.1007/3-540-40021-4_1.
- Carvalho CM, Aires-Barros MR, Cabral JMS. 1999. Cutinase: from molecular level to bioprocess development. *Biotechnol Bioeng* 66: 17–34. [https://doi.org/10.1002/\(SICI\)1097-0290\(1999\)66:1<17::AID-BIT2>3.0.CO;2-F](https://doi.org/10.1002/(SICI)1097-0290(1999)66:1<17::AID-BIT2>3.0.CO;2-F).
- Soliday CL, Flurkey WH, Okita TW, Kolattukudy PE. 1984. Cloning and structure determination of cDNA for cutinase, an enzyme involved in fungal penetration of plants. *Proc Natl Acad Sci U S A* 81:3939–3943. <https://doi.org/10.1073/pnas.81.13.3939>.
- Skamnioti P, Gurr SJ. 2008. Cutinase and hydrophobin interplay. *Plant Signal Behav* 3:248–250. <https://doi.org/10.4161/psb.3.4.5181>.
- Martinez C, de Geus P, Lauwereys M, Matthysse G, Cambillau C. 1992. *Fusarium solani* cutinase is a lipolytic enzyme with a catalytic serine accessible to solvent. *Nature* 356:615–618. <https://doi.org/10.1038/356615a0>.
- Ollis DL, Cheah E, Cygler M, Dijkstra B, Frolov F, Franken SM, Harel M, Remington SJ, Silman I, Schrag J, Sussman JL, Verschueren KHG, Goldman A. 1992. The α/β hydrolase fold. *Protein Eng* 5:197–211. <https://doi.org/10.1093/protein/5.3.197>.
- Rauwerdink A, Kazlauskas RJ. 2015. How the same core catalytic machinery catalyzes 17 different reactions: the serine-histidine-aspartate catalytic triad of α/β -hydrolase fold enzymes. *ACS Catal* 5:6153–6176. <https://doi.org/10.1021/acscatal.5b01539>.
- Khan FI, Lan D, Durrani R, Huan W, Zhao Z, Wang Y. 2017. The lid domain in lipases: structural and functional determinant of enzymatic properties. *Front Bioeng Biotechnol* 5:16. <https://doi.org/10.3389/fbioe.2017.00016>.
- Chen S, Tong X, Woodard RW, Du G, Wu J, Chen J. 2008. Identification and characterization of bacterial cutinase. *J Biol Chem* 283:25854–25862. <https://doi.org/10.1074/jbc.M800848200>.
- Acero EH, Doris A, Georg R, Steinkellner G, Gruber K, Greimel K, Eiteljörg I, Trotscha E, Wei R, Zimmermann W, Zinn M, Cavaco-Paulo A, Freddi G, Schwab H, Guebitz G. 2011. Enzymatic surface hydrolysis of PET: effect of structural diversity on kinetic properties of cutinases from *Thermobifida*. *Macromolecules* 44:4632–4640. <https://doi.org/10.1021/ma200949p>.
- Ribitsch D, Acero EH, Greimel K, Eiteljörg I, Trotscha E, Freddi G, Schwab H, Guebitz GM. 2012. Characterization of a new cutinase from *Thermobifida alba* for PET-surface hydrolysis. *Biocatal Biotransformation* 30:2–9. <https://doi.org/10.3109/10242422.2012.644435>.
- Thumarat U, Nakamura R, Kawabata T, Suzuki H, Kawai F. 2012. Biochemical and genetic analysis of a cutinase-type polyesteresterase from a thermophilic *Thermobifida alba* AHK119. *Appl Microbiol Biotechnol* 95:419–430. <https://doi.org/10.1007/s00253-011-3781-6>.
- Wei R, Oeser T, Then J, Kühn N, Barth M, Schmidt J, Zimmermann W. 2014. Functional characterization and structural modeling of synthetic polyester-degrading hydrolases from *Thermomonospora curvata*. *AMB Express* 4:44. <https://doi.org/10.1186/s13568-014-0044-9>.
- Sulaiman S, You DJ, Kanaya E, Koga Y, Kanaya S. 2014. Crystal structure and thermodynamic and kinetic stability of metagenome-derived LC-cutinase. *Biochemistry* 53:1858–1869. <https://doi.org/10.1021/bi401561p>.
- Nikolaivits E, Kanelli M, Dimarogona M, Topakas E. 2018. A middle-aged enzyme still in its prime: recent advances in the field of cutinases. *Catalysts* 8:612. <https://doi.org/10.3390/catal8120612>.
- West NP, Chow PME, Randall EJ, Wu J, Chen J, Ribeiro JMC, Britton WJ. 2009. Cutinase-like proteins of *Mycobacterium tuberculosis*: characterization of their variable enzymatic functions and active site identification. *FASEB J* 23:1694–1704. <https://doi.org/10.1096/fj.08-114421>.
- Chen S, Su L, Chen J, Wu J. 2013. Cutinase: characteristics, preparation and applications. *Biotechnol Adv* 31:1754–1767. <https://doi.org/10.1016/j.biotechadv.2013.09.005>.
- Ronkvist AM, Xie W, Lu W, Gross RA. 2009. Cutinase-catalyzed hydrolysis of poly(ethylene terephthalate). *Macromolecules* 42:5128–5138. <https://doi.org/10.1021/ma9005318>.
- Liu Z, Gosser Y, Baker PJ, Ravee Y, Lu Z, Alemu G, Li H, Butterfoss GL, Kong X-P, Gross R, Montclare JK. 2009. Structure and functional studies of *Aspergillus oryzae* cutinase: enhanced thermostability and hydrolytic activity of synthetic ester and polyester degradation. *J Am Chem Soc* 131: 15711–15716. <https://doi.org/10.1021/ja9046697>.
- Taniguchi I, Yoshida S, Hiraga K, Miyamoto K, Kimura Y, Oda K. 2019. Bio-degradation of PET: current status and application aspects. *ACS Catal* 9: 4089–4105. <https://doi.org/10.1021/acscatal.8b05171>.
- Urbanek AK, Mirończuk AM, Garcia-Martin A, Saborido A, de la Mata I, Arroyo M. 2020. Biochemical properties and biotechnological applications of microbial enzymes involved in the degradation of polyester-type plastics. *Biochim Biophys Acta Proteins Proteom* 1868:140315. <https://doi.org/10.1016/j.bbapap.2019.140315>.
- Dutta K, Sen S, Veeranki VD. 2009. Production, characterization and applications of microbial cutinases. *Process Biochem* 44:127–134. <https://doi.org/10.1016/j.procbio.2008.09.008>.
- Guebitz GM, Cavaco-Paulo A. 2008. Enzymes go big: surface hydrolysis and functionalization of synthetic polymers. *Trends Biotechnol* 26:32–38. <https://doi.org/10.1016/j.tibtech.2007.10.003>.
- Pio TF, Macedo GA. 2009. Cutinases: properties and industrial applications. *Adv Appl Microbiol* 66:77–95. [https://doi.org/10.1016/S0065-2164\(08\)00804-6](https://doi.org/10.1016/S0065-2164(08)00804-6).
- Su A, Tyrikos-Ergas T, Shirke AN, Zou Y, Dooley AL, Pavlidis IV, Gross RA. 2018. Revealing cutinases' capabilities as enantioselective catalysts. *ACS Catal* 8:7944–7951. <https://doi.org/10.1021/acscatal.8b02099>.
- Nyyssola A. 2015. Which properties of cutinases are important for applications? *Appl Microbiol Biotechnol* 99:4931–4942. <https://doi.org/10.1007/s00253-015-6596-z>.
- Bagwell CE, Bhat S, Hawkins GM, Smith BW, Biswas T, Hoover TR, Saunders E, Han CS, Tsodikov OV, Shimkets LJ. 2008. Survival in nuclear waste, extreme resistance, and potential applications gleamed from the genome sequence of *Kineococcus radiotolerans* SRS30216. *PLoS One* 3: e3878. <https://doi.org/10.1371/journal.pone.0003878>.
- Copeland A, Lucas S, Lapidus A, Barry K, Glavina del Rio T, Hammon N, Israni S, Dalin E, Tice H, Pitluck S, Saunders E, Brettin T, Bruce D, Detter JC, Han C, Schmutz J, Larimer F, Land M, Hauser L, Kyridis N, Lykidis A, Bagwell CE, Shimkets L, Berry CJ, Fliermans C, Richardson P. 2007. Data from "Complete sequence of chromosome of *Kineococcus radiotolerans* SRS30216." GenBank <https://www.ncbi.nlm.nih.gov/nucleotide/CP000750.2/> (accession number CP000750.2).
- Hiraishi T, Hirahara Y, Doi Y, Maeda M, Taguchi S. 2006. Effects of mutations in the substrate-binding domain of poly[(R)-3-hydroxybutyrate] (PHB) depolymerase from *Ralstonia pickettii* T1 on PHB degradation. *Appl Environ Microbiol* 72:7331–7338. <https://doi.org/10.1128/AEM.01187-06>.
- Morohoshi T, Oi T, Suzuki T, Sato S. 2020. Identification and characterization of a novel extracellular polyhydroxyalkanoate depolymerase in the complete genome sequence of *Undibacterium* sp. KW1 and YM2 strains. *PLoS One* 15:e0232698. <https://doi.org/10.1371/journal.pone.0232698>.
- Belbahri L, Calmin G, Mauch F, Andersson JO. 2008. Evolution of the cutinase gene family: evidence for lateral gene transfer of a candidate *Phytophthora* virulence factor. *Gene* 408:1–8. <https://doi.org/10.1016/j.gene.2007.10.019>.
- Waterhouse A, Bertoni M, Bienert S, Studer G, Tauriello G, Gumienny R, Heer FT, de Beer TAP, Rempfer C, Bordoli LS, Lepore R, Schwede T. 2018. SWISS-MODEL: homology modelling of protein structures and complexes. *Nucleic Acids Res* 46:W296–W303. <https://doi.org/10.1093/nar/gky427>.
- Zhang G, Brokx S, Weiner JH. 2006. Extracellular accumulation of recombinant proteins fused to the carrier protein YebF in *Escherichia coli*. *Nat Biotechnol* 24:100–104. <https://doi.org/10.1038/nbt1174>.
- Xiao Z, Bergeron H, Grosse S, Beauchemin M, Garron ML, Shaya D, Sulea T, Cygler M, Lau PCK. 2008. Improvement of the thermostability and activity of a pectate lyase by single amino acid substitutions, using a strategy based on melting-temperature-guided sequence alignment. *Appl Environ Microbiol* 74:1183–1189. <https://doi.org/10.1128/AEM.02220-07>.
- Biswas T, Pero JM, Joseph CG, Tsodikov CV. 2009. DNA-dependent ATPase activity of bacterial XPB helicases. *Biochemistry* 48:2839–2848. <https://doi.org/10.1021/bi8022416>.
- Phillips RW, Wiegel J, Berry CJ, Fliermans C, Peacock AD, White DC, Shimkets LJ. 2002. *Kineococcus radiotolerans* sp. nov., a radiation-resistant, Gram-positive bacterium. *Int J Syst Evol Microbiol* 52:933–938. <https://doi.org/10.1099/00207713-52-3-933>.
- Gao N, Ma B-G, Zhang Y-S, Song Q, Chen L-L, Zhang H-Y. 2009. Gene expression analysis of four radiation-resistant bacteria. *Genomics Insights* 2:11–22. <https://doi.org/10.4137/gei.s2380>.
- Chen Z, Li L, Shan Z, Huang H, Chen H, Ding X, Guo J, Liu L. 2016. Transcriptome sequencing analysis of novel sRNAs of *Kineococcus radiotolerans* in response to ionizing radiation. *Microbiol Res* 192:122–129. <https://doi.org/10.1016/j.micres.2016.06.001>.
- Jendrossek D, Handrick R. 2002. Microbial degradation of polyhydroxyalcanoates. *Annu Rev Microbiol* 53:403–432. <https://doi.org/10.1146/annurev.micro.53.012302.160838>.

41. Kwon M, Kim HS, Yang TH, Song BK, Song JK. 2009. High-level expression and characterization of *Fusarium solani* cutinase in *Pichia pastoris*. *Protein Expr Purif* 68:104–109. <https://doi.org/10.1016/j.pep.2009.06.021>.
42. Prehna G, Zhang G, Gong X, Duszyk M, Okon M, McIntosh LP, Weiner JH, Strynadka NCJ. 2012. A protein export pathway involving *Escherichia coli* porins. *Structure* 20:1154–1166. <https://doi.org/10.1016/j.str.2012.04.014>.
43. Horler RSP, Butcher A, Papangelopoulos N, Ashton PD, Thomas GH. 2009. EchoLocation: an *in silico* analysis of the subcellular locations of *Escherichia coli* proteins and comparison with experimentally derived locations. *Bioinformatics* 25:163–166. <https://doi.org/10.1093/bioinformatics/btn596>.
44. Olsen JV, Ong SE, Mann M. 2004. Trypsin cleaves exclusively C-terminal to arginine and lysine residues. *Mol Cell Proteomics* 3:608–614. <https://doi.org/10.1074/mcp.T400003-MCP200>.
45. Su L, Hong R, Wu J. 2015. Enhanced extracellular expression of gene-optimized *Thermobifida fusca* cutinase in *Escherichia coli* by optimization of induction strategy. *Process Biochem* 50:1039–1046. <https://doi.org/10.1016/j.procbio.2015.03.023>.
46. Duan X, Liu Y, You X, Jiang Z, Yang S, Yang S. 2017. High-level expression and characterization of a novel cutinase from *Malbranchea cinnamomea* suitable for butyl butyrate production. *Biotechnol Biofuels* 10:223. <https://doi.org/10.1186/s13068-017-0912-z>.
47. Longhi S, Cambillau C. 1999. Structure-activity of cutinase, a small lipolytic enzyme. *Biochim Biophys Acta* 1441:185–196. [https://doi.org/10.1016/s1388-1981\(99\)00159-6](https://doi.org/10.1016/s1388-1981(99)00159-6).
48. Matak MY, Moghaddam ME. 2009. The role of short-range Cys171-Cys178 disulfide bond in maintaining cutinase active site integrity: a molecular dynamics simulation. *Biochem Biophys Res Commun* 390:201–204. <https://doi.org/10.1016/j.bbrc.2009.09.073>.
49. Chen S, Wu Y, Su L, Wu J. 2019. Contribution of disulfide bond to the stability of *Thermobifida fusca* cutinase. *Food Biosci* 27:6–10. <https://doi.org/10.1016/j.fbio.2018.11.001>.
50. Bollinger A, Thies S, Knieps-Grünhagen E, Gertzen C, Kobus S, Höppner A, Ferrer M, Gohlke H, Smits SHJ, Jaeger K-E. 2020. A novel polyester hydrolase from the marine bacterium *Pseudomonas aestuansnigri*—structural and functional insights. *Front Microbiol* 11:114. <https://doi.org/10.3389/fmicb.2020.00114>.
51. Kawai F. 2021. The current state of research on PET hydrolyzing enzymes available for biorecycling. *Catalysts* 11:206. <https://doi.org/10.3390/catal11020206>.
52. Kasuya K, Ohura T, Masuda K, Doi Y. 1999. Substrate and binding specificities of bacterial polyhydroxybutyrate depolymerases. *Int J Biol Macromol* 24:329–336. [https://doi.org/10.1016/s0141-8130\(99\)00046-x](https://doi.org/10.1016/s0141-8130(99)00046-x).
53. Poon DKY, Withers SG, McIntosh LP. 2007. Direct demonstration of the flexibility of the glycosylated proline-threonine linker in the *Cellulomonas fimi* xylanase Cex through NMR spectroscopic analysis. *J Biol Chem* 282: 2091–2100. <https://doi.org/10.1074/jbc.M609670200>.
54. Halonen P, Reinikainen T, Nyysöla A, Buchert J. 2009. A high throughput profiling method for cutinolytic esterases. *Enzyme Microb Technol* 44: 394–399. <https://doi.org/10.1016/j.enzmictec.2008.12.012>.
55. Kim Y-H, Lee J, Moon SH. 2003. Uniqueness of microbial cutinases in hydrolysis of *p*-nitrophenyl esters. *J Microbiol Biotechnol* 13:57–63.
56. Gerard HC, Fett WF, Osann SF, Moreau RA. 1993. Evaluation of cutinase activity of various industrial lipases. *Biotechnol Appl Biochem* 17:181–189.
57. Murphy CA, Cameron JA, Huang SJ, Vinopal RT. 1996. *Fusarium* polycaprolactone depolymerase is cutinase. *Appl Environ Microbiol* 62:456–460. <https://doi.org/10.1128/aem.62.2.456-460.1996>.
58. Baker PJ, Poultney C, Liu Z, Gross R, Montclare JK. 2012. Identification and comparison of cutinases for synthetic polyester degradation. *Appl Microbiol Biotechnol* 93:229–240. <https://doi.org/10.1007/s00253-011-3402-4>.
59. Shi K, Jing J, Song L, Su T, Wang Z. 2020. Enzymatic hydrolysis of polyester degradation of poly(*ε*-caprolactone) by *Candida antarctica* lipase and *Fusarium solani* cutinase. *Int J Biol Macromol* 144:183–189. <https://doi.org/10.1016/j.ijbiomac.2019.12.105>.
60. Butbunchu N, Pathom-Aree W. 2019. Actinobacteria as promising candidate for polylactic acid type bioplastic degradation. *Front Microbiol* 10: 2834. <https://doi.org/10.3389/fmicb.2019.02834>.
61. Degani O, Gepstein S, Dosoretz CG. 2002. Potential use of cutinase in enzymatic scouring of cotton fiber cuticle. *Appl Biochem Biotechnol* 102-103:277–289. <https://doi.org/10.1385/ABAB:102-103:1-6:277>.
62. Degani O. 2021. Synergism between cutinase and pectinase in the hydrolysis of cotton fibers' cuticle. *Catalysts* 11:84. <https://doi.org/10.3390/catal11010084>.
63. Agrawal PB, Agrawal PB, Nierstrasz VA, Bouwhuis GH, Warmoeskerken MMCG. 2008. Cutinase and pectinase in cotton bioscouring: an innovative and fast bioscouring process. *Enzyme Microb Technol* 26:412–421. <https://doi.org/10.1080/10242420802332558>.
64. Agrawal PB, Nierstrasz VA, Warmoeskerken MMCG. 2008. Role of mechanical action in low-temperature cotton scouring with *F. solani pisi* cutinase and pectate lyase. *Enzyme Microb Technol* 42:473–482. <https://doi.org/10.1016/j.enzmictec.2008.01.016>.
65. Akin DE, Condon B, Sohn M, Foulk JA, Dodd RB, Rigsby LL. 2007. Optimization for enzyme retting of flax with pectate lyase. *Ind Crops Prod* 25: 136–146. <https://doi.org/10.1016/j.indcrop.2006.08.003>.
66. Shanahan ER, Pinto R, Triccas JA, Britton WJ, West NP. 2010. Cutinase-like protein-6 of *Mycobacterium tuberculosis* is recognized in tuberculosis patients and protects mice against pulmonary infection as a single and fusion protein vaccine. *Vaccine* 28:1341–1346. <https://doi.org/10.1016/j.vaccine.2009.11.010>.
67. Strong EJ, West NP. 2018. Use of soluble extracellular regions of MmpL (SERoM) as vaccines for tuberculosis. *Sci Rep* 8:5604. <https://doi.org/10.1038/s41598-018-23893-3>.
68. Harwood C, Buckley M. 2008. The uncharted microbial world: microbes and their activities in the environment. American Society for Microbiology, Washington, DC.
69. Sambrook J, Fritsch EF, Maniatis T. 1989. Molecular cloning: a laboratory manual, 2nd ed. Cold Spring Harbor Laboratory Press, Cold Spring Harbor, NY.
70. Smith PK, Krohn RI, Hermanson GT, Mallia AK, Gartner FH, Provenzano EK, Fujimoto EK, Goede NM, Olson BJ, Klenk DC. 1985. Measurement of protein using bicinchoninic acid. *Anal Biochem* 150:76–85. [https://doi.org/10.1016/0003-2697\(85\)90442-7](https://doi.org/10.1016/0003-2697(85)90442-7).
71. Whelan S, Goldman N. 2001. A general empirical model of protein evolution derived from multiple protein families using a maximum-likelihood approach. *Mol Biol Evol* 18:691–699. <https://doi.org/10.1093/oxfordjournals.molbev.a003851>.
72. Kumar S, Stecher G, Tamura K. 2016. MEGA7: molecular evolutionary genetics analysis version 7.0 for bigger datasets. *Mol Biol Evol* 33: 1870–1874. <https://doi.org/10.1093/molbev/msw054>.
73. Pitt D. 1988. Pectin lyase from *Phoma medicaginis* var. *pinodella*. *Methods Enzymol* 161:350–352. [https://doi.org/10.1016/0076-6879\(88\)61039-1](https://doi.org/10.1016/0076-6879(88)61039-1).